Comparison between SSF and Critical-Plane Models to Predict Fatigue Lives under Multiaxial Proportional Histories

M. de Freitas[1], L. Reis[1], M.A. Meggiolaro[2] and J.T.P. de Castro[2]

[1] IDMEC, Instituto Superior Técnico, Av. Rovisco Pais, 1049-001 Lisboa, Portugal, mfreitas@dem.ist.utl.pt, luis.g.reis@ist.utl.pt

[2] Pontifical Catholic University of Rio de Janeiro, PUC-Rio, Rua Marquês São Vicente, Rio de Janeiro, RJ, 22451-900, Brazil, meggi@puc-rio.br, jtcastro@puc-rio.br

ABSTRACT. *Materials can be classified as shear or tensile sensitive, depending on the main fatigue microcrack initiation process under multiaxial loadings. The nature of the initiating microcrack can be evaluated from a stress scale factor (SSF), which usually multiplies the hydrostatic or the normal stress term from the adopted multiaxial fatigue damage parameter. Low SSF values are associated with a shear-sensitive material, while a large SSF indicates that a tensile-based model should be used instead. For tension-torsion histories, a recent published approach combines the shear and normal stress amplitudes using a SSF polynomial function that depends on the stress amplitude ratio (SAR) between the shear and normal components. Alternatively, critical-plane models calculate damage on the plane where damage is maximized, adopting a SSF value that is assumed constant for a given material, sometimes varying with the fatigue life (in cycles), but not with the SAR, the stress amplitude level, or the loading path shape. In this work, in-phase proportional tension-torsion tests in 42CrMo4 steel specimens for several values of the SAR are presented. The SSF approach is then compared with critical-plane models, based on their predicted fatigue lives and the observed values for the studied tension-torsion histories.*

INTRODUCTION

Initiating microcracks under multiaxial loading are usually sub-divided into shear or tensile types [1]. The dominant fatigue mechanism in so-called shear-sensitive materials is Mode II microcrack nucleation in shear, in directions that maximize the ranges of the shear components, with the normal components only playing a secondary role.

However, other materials may initiate fatigue cracks on planes of maximum tensile strain or stress ranges, such as 304 stainless steel under certain load histories, and cast irons; in this case, even if the microcrack nucleates in shear, its so-called initiation life (which always includes some microcrack propagation) is controlled by its growth in a direction perpendicular to the maximum principal stress or strain. Moreover, a material can be shear-sensitive for short, but tensile-sensitive for long fatigue lives, a behavior that can depend as well on the loading type.

The shear or tensile nature of the initiating microcrack can be evaluated from a stress scale factor (SSF), which usually multiplies the hydrostatic or the normal stress term from the adopted multiaxial fatigue damage parameter. Low values of the SSF indicate a shear-sensitive material, which usually requires shear-based damage models such as Findley's [2] or Fatemi-Socie's [3]; on the other hand, large SSF values indicate that a tensile-based model should be used instead, like Smith-Watson-Topper's [4].

The approach proposed by Anes et al [5], for tension-torsion histories, combines the shear and normal stress amplitudes applied on the specimen cross section, using a SSF polynomial function that depends on the SAR between shear and normal components. Alternatively, the critical-plane approach calculates damage on the plane where damage is maximized (not on the plane where the load is applied), while adopting a SSF value that is assumed constant for a given material, sometimes varying with the fatigue life (in cycles), but not with the SAR, stress amplitude level, or loading path shape.

In this work, in-phase proportional tension-torsion tests are conducted in 42CrMo4 steel specimens for several values of the SAR. The SSF and critical-plane approaches are then compared, based on their predicted fatigue lives and the experimentally measured ones.

SSF EQUIVALENT SHEAR STRESS APPROACH

The SSF equivalent shear stress approach, proposed in [5], considers that both the SAR and the stress loading level significantly influence the material fatigue strength. Such effects were accounted for through the SSF function, which transforms an axial damage into a shear one. With this equivalent stress, it is also possible to estimate fatigue lives N_f, using the uniaxial shear stress SN curve represented as

$$\max_{block}\left(\tau + ssf \cdot \sigma\right) = A\left(N_f\right)^b. \tag{1}$$

$$ssf\left(\sigma_a,\lambda\right) = a + b\cdot\sigma_a + c\cdot\sigma_a^2 + d\cdot\sigma_a^3 + f\cdot\lambda^2 + g\cdot\lambda^3 + h\cdot\lambda^4 + i\cdot\lambda^5. \tag{2}$$

where σ_a and τ_a are respectively the amplitude of the axial and shear component of the tension-torsion loading, and $\lambda \equiv \tan^{-1}(\tau_a/\sigma_a)$ is the SAR. The constants from "a" to "i" are determined through experimental tests, therefore the SSF function is a material fatigue property and must be determined from experimental tests.

CRITICAL-PLANE APPROACH

The critical-plane approach assumes that fatigue lives can be calculated from the damage at the critical plane of the critical point. It also assumes that damage on all other planes do not influence the initiation of the microcrack. Here, the main calculation challenge is to compute the accumulated damage in many candidate planes at the

critical point, to find the direction of the critical one where it is maximized (and thus where the crack is expected to initiate). This search is very much simplified for in-phase proportional constant amplitude load histories, such as the ones studied in this work.

Findley's shear model

Findley explicitly introduced the critical plane idea [2], proposing a stress-based fatigue damage model applicable to multiaxial loads. Such models assume that the fatigue crack initiates at the component's critical point on its critical plane, where a suitable damage parameter is maximized. This is physically sensible and considers in a very reasonable way how the fatigue cracking process works under multiaxial loads in those materials.

Findley assumed fatigue damage is caused by the parameter $[\Delta\tau/2 + \alpha_F\cdot\sigma_{\perp max}]$, which combines the shear stress range $\Delta\tau/2$ acting on the critical plane with the peak of the normal stress perpendicular ($\perp$) to that plane $\sigma_{\perp max}$, during the considered load event. In this way, fatigue cracking would take place at the critical point in directions where this reasonable damage parameter is maximized.

For a Case A candidate plane, which is perpendicular to the free surface and makes an angle θ with the x axis, Findley's infinite-life criterion (for multiaxial fatigue under any type of loading) is given by the maximization problem

$$\max_{\theta}\left[\Delta\tau_A(\theta)/2 + \alpha_F\cdot\sigma_{\perp max}(\theta)\right] = \beta_F \tag{3}$$

where Findley's coefficient α_F and shear fatigue limit β_F must be calibrated from measurements in at least two types of fatigue tests, e.g. under rotary bending and cyclic torsion, or else under push-pull tests at $R = \sigma_{min}/\sigma_{max} = 0$ and $R = -1$.

Findley's infinite-life model from Eq. 3 can be extended to finite-life calculations using a shear version of Wöhler's curve, equating Findley's fatigue limit β_F with the torsional fatigue limit τ_L, resulting in

$$\max_{\theta}\left[\frac{\Delta\tau_A(\theta)}{2} + \alpha_F\cdot\sigma_{\perp max}(\theta)\right] = \frac{\beta_F}{\tau_L}\cdot\tau_c\cdot(2N)^{b_\tau} \tag{4}$$

where τ_c and b_τ are the torsional strength coefficient and exponent, respectively, calibrated under pure torsion. For the studied in-phase tension-torsion history, Findley's predicted fatigue life N_F (in cycles) becomes after some algebraic manipulation

$$\sqrt{\sigma_a{}^2 + 4\tau_a{}^2} + \frac{\alpha_F}{\sqrt{1+\alpha_F{}^2}}\cdot\sigma_a = \frac{2\beta_F}{\tau_L\sqrt{1+\alpha_F{}^2}}\cdot\tau_c\cdot(2N_F)^{b_\tau} \tag{5}$$

Therefore, N_F can be obtained as a function of σ_a and τ_a.

Smith-Watson-Topper's tensile model

Findley's or Fatemi-Socie's model are not appropriate for tensile-sensitive materials, where Case A tensile cracks initiate. In these materials, the fatigue initiation life N of such cracks must be correlated with a damage parameter based on a normal range $\Delta\varepsilon_\perp$ (not on a shear range $\Delta\gamma$), combined with the peak stress $\sigma_{\perp max}$ parallel to $\varepsilon_\perp$ to account for mean/maximum stress effects.

The multiaxial version of Smith-Watson-Topper's (SWT) model [4] is particularly useful for calculating the fatigue damage of such materials, especially if the propagation phase of the microcracks (still within the so-called crack initiation stage), which is more sensitive to the normal stresses, is dominant over its shear-controlled initiation. The multiaxial version of SWT's equation for Case A tensile cracks can be written as

$$\max_\theta \left(\sigma_{\perp max}(\theta) \cdot \frac{\Delta\varepsilon_\perp(\theta)}{2} \right) = \frac{\sigma_c^2}{E}(2N)^{2b} + \sigma_c \varepsilon_c (2N)^{b+c} \tag{6}$$

where σ_c, ε_c, b and c are Coffin-Manson's material parameters.

In high-cycle fatigue calculations, an elastic version ESWT of the SWT model can be adopted. Under linear-elastic uniaxial conditions, the plastic term $\sigma_c \varepsilon_c (2N)^{b+c}$ in Eq. 6 can be neglected, while Hooke's law gives $\Delta\sigma_\perp(\theta)/2 = E \cdot \Delta\varepsilon_\perp(\theta)/2$, resulting in

$$ESWT = \max_\theta \left(\sigma_{\perp max}(\theta) \cdot \frac{\Delta\sigma_\perp(\theta)}{2} \right) = \sigma_c^2 (2N)^{2b} \tag{7}$$

This equation can be simplified in the studied proportional history (which has zero mean stresses), because in this fully-alternate case the peak normal stress $\sigma_{\perp max}(\theta)$ perpendicular to a Case A plane along θ is equal to the normal amplitude $\Delta\sigma_\perp(\theta)/2$. Therefore, the ESWT equation becomes Wöhler's curve using Basquin's formulation:

$$\max_\theta \left(\sigma_{\perp max}(\theta) \cdot \frac{\Delta\sigma_\perp(\theta)}{2} \right) = \max_\theta \left[\left(\frac{\Delta\sigma_\perp(\theta)}{2} \right)^2 \right] = \sigma_c^2 (2N)^{2b} \Rightarrow \max_\theta \left(\frac{\Delta\sigma_\perp(\theta)}{2} \right) = \sigma_c (2N)^b \tag{8}$$

Thus, the damage parameter to be maximized in the ESWT model simply becomes $\Delta\sigma_\perp(\theta)/2 = |\sigma_a \cdot \cos^2\theta + \tau_a \sin 2\theta|$ for a fully-alternate cyclic loading. Deriving this expression and equating it to zero, the critical-plane angle θ_{ESWT} with respect to the x axis, represented in the first quadrant $0º \leq \theta \leq 90º$, is obtained from

$$-\sigma_a \cdot 2\cos\theta\sin\theta + 2\tau_a \cos 2\theta = 0 \Rightarrow \tan 2\theta_{ESWT} = \frac{2\tau_a}{\sigma_a} = \tan 2\theta_p = 2\tan\lambda \tag{9}$$

where λ is the SAR from the SSF model [5], and θ_p is the principal direction from the first quadrant. Not surprisingly, θ_{ESWT} is one of the fixed principal directions θ_p of such

proportional tension-torsion loadings. On this principal plane, the damage parameter is maximized, resulting in the principal stress equation for the normal and shear amplitudes σ_a and τ_a:

$$\frac{\Delta\sigma_\perp(\theta_{ESWT})}{2} = \sigma_a\frac{1+\cos 2\theta_{ESWT}}{2} + \tau_a\sin 2\theta_{ESWT} = \frac{\sigma_a+\sqrt{\sigma_a{}^2+4\tau_a{}^2}}{2} \qquad (10)$$

From the definition $\lambda \equiv \tan^{-1}(\tau_a/\sigma_a)$, it follows that $\tau_a = \sigma_a\cdot\tan(\lambda)$, thus this maximized damage parameter on the θ_{ESWT} plane can be expressed as a function of σ_a and λ:

$$\frac{\Delta\sigma_\perp(\theta_{ESWT})}{2} = \frac{\sigma_a+\sqrt{\sigma_a{}^2+4\sigma_a{}^2\tan^2\lambda}}{2} = \sigma_a\cdot\left[0.5+\sqrt{0.25+\tan^2\lambda}\right] \qquad (11)$$

Assuming ESWT's model is able to predict crack initiation, the above expression would explain why the SSF can be represented as a function of σ_a and λ, however requiring a fifth-order polynomial function to approximately reproduce such a non-linear expression. Finally, from the ESWT equation it follows that the predicted fatigue life N_{ESWT} (in cycles) is

$$N_{ESWT} = 0.5\cdot\left[\frac{\Delta\sigma_\perp(\theta_{ESWT})}{2\sigma_c}\right]^{1/b} = 0.5\cdot\left[\frac{\sigma_a+\sqrt{\sigma_a{}^2+4\tau_a{}^2}}{2\sigma_c}\right]^{1/b} = 0.5\cdot\left[\frac{\sigma_a}{\sigma_c}\cdot\left(0.5+\sqrt{0.25+\tan^2\lambda}\right)\right]^{1/b} \quad (12)$$

RESULTS AND DISCUSSION

Material and loading paths

The reasoning derived in the previous sections is applied to the experimental results available in Anes et al. [5] for multiaxial fatigue tests carried out in low-alloy steel 42CrMo4. These metal alloys are heat-treated by austenitizing, quenching, and tempering to improve their mechanical properties. The chemical composition and the monotonic and cyclic properties of 42CrMo4 are available in [5, 6].

Fatigue tests are carried out through a servo-hydraulic tension-torsion machine under stress control at room temperature, applying proportional loading paths. In order to perform the SSF mapping, five different proportional loading paths are selected with different SAR λ. Although the SAR is an important fatigue variable, the stress level also has a high influence on the fatigue damage mechanisms. These two variables will be used in the SSF mapping.

Life prediction

The tested 42CrMo4 steel has Young's modulus, Coffin-Manson's fatigue strength coefficient and exponent, and Coffin-Manson's fatigue ductility coefficient and exponent presented in Freitas et al [6]. But the ESWT model adopts an elastic version of

Coffin-Manson's equation, which neglects its plastic term. Therefore, the resulting purely-elastic calibration requires a better fit of the experimental data to also account for lower fatigue lives. From the normal and shear fittings, it is possible to write:

$$\sigma_a = \sigma_c \cdot (2N)^b = 1654 \cdot (2N)^{-0.0934} \quad \text{and} \quad \tau_a = \tau_c \cdot (2N)^{b_\tau} = 911 \cdot (2N)^{-0.0623} \qquad (13)$$

Then, from Findley's calibration for Case A cracks, from Eq. 3, its constants can be determined: $\alpha_F = 0.668$ and $\beta_F = 420.9$ MPa.

Figs. 1-3 present a comparison between the observed fatigue lives N_{obsv} and the N_{SSF}, N_{ESWT} and N_F predicted by the SSF, ESWT and Findley's methods, respectively, for SAR $\lambda = 0°$ (uniaxial), 30°, 45°, 60° and 90° (pure torsion). As observed in Fig. 1, the polynomial fitting of the SSF expression was well performed, allowing a good match between N_{obsv} and N_{SSF} for all cases.
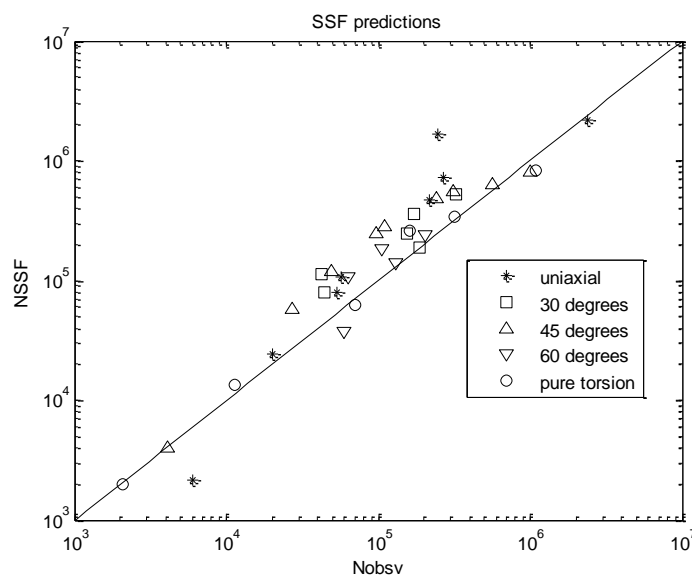

Figure 1. Comparison between the observed fatigue lives N_{obsv} and the fitted N_{SSF}.

As shown in Fig. 2, ESWT's critical-plane method results in reasonable fatigue life predictions, except for the pure torsion ($\lambda = 90°$) case. This result suggests that the pure torsion history involved significant shear damage, as expected, however ESWT's model only accounts for tensile damage.

Findley's critical-plane method also results in reasonable fatigue life predictions, except for the $\lambda = 30°$ and $\lambda = 45°$ cases, as shown in Fig. 3. This suggests that these histories involved significant tensile damage, however Findley's model only accounts for shear damage. The maximum normal stress $\sigma_{\perp max}$ influences Findley's shear damage parameter, however no measure of the normal range $\Delta\sigma_\perp$ perpendicular to the critical plane is considered. Nevertheless, Findley's predictions for the uniaxial case are surprisingly good, indicating that at least in this in-phase zero-mean proportional case the $\sigma_{\perp max}$ term was able to capture the damaging $\Delta\sigma_\perp$ effects.

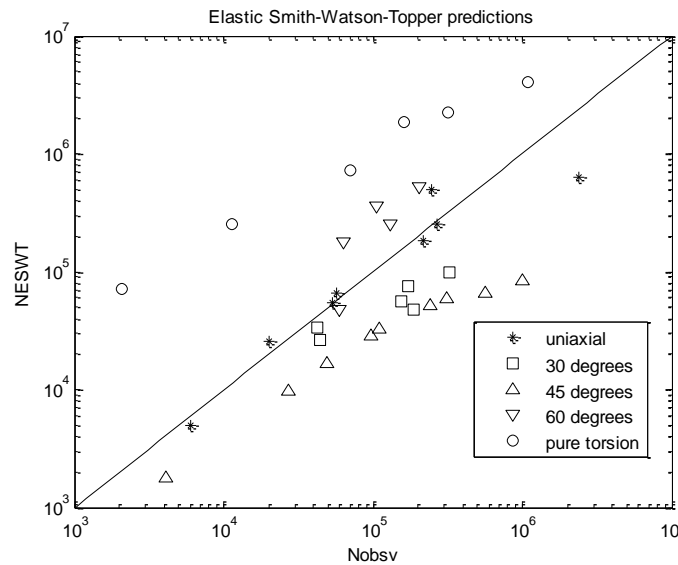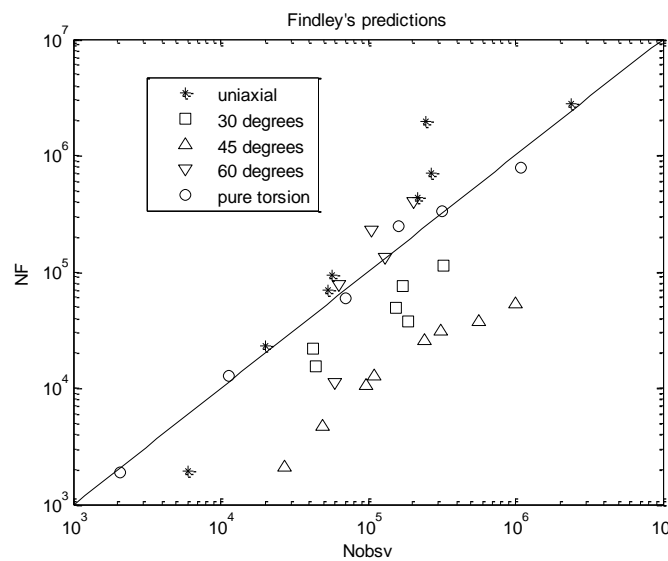Figure 2. Comparison between the observed fatigue lives N_{obsv} and the predicted N_{ESWT}.

Figure 3. Comparison between the observed fatigue lives N_{obsv} and the predicted N_F.

Figure 4 shows critical-plane predictions based on ESWT's tensile model applied to the predominantly tensile cases $\lambda = 0°$ (uniaxial), $30°$, and $45°$; and on Findley's shear model to the shear-dominated cases $\lambda = 60°$ and $90°$ (pure torsion). Notice that the prediction scatter is similar to the one from the SSF method. However, such critical-plane method calculations have a greater prediction potential, because they were only based on curve fittings of the uniaxial and pure-torsion experiments, while the polynomial from the SSF method required data calibration from all five tests.
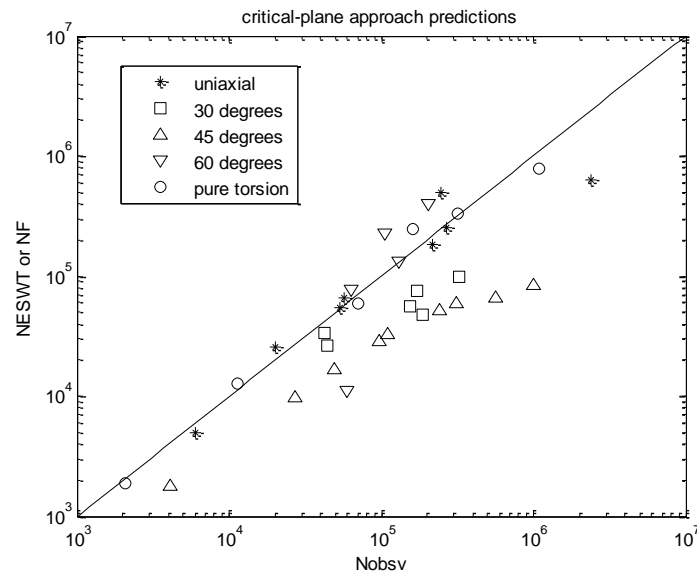
Figure 4. Comparison between the observed lives N_{obsv} and the N_{ESWT} or N_F predicted by critical-plane methods, according to dominance of normal or shear applied loads.

CONCLUSIONS

In this work, it was shown that both critical-plane and SSF approaches have the potential to predict multiaxial fatigue lives, at least for in-phase proportional loadings. Findley's model neglects tensile damage, while the ESWT model neglects shear damage, which explains why their performance was not very good for all considered load histories. In its current form, the SSF method does not include mean/maximum stress effects, therefore experiments with zero mean loads were chosen to evaluate its performance. The SSF method resulted in a better fit of the experimental data, however it requires more calibration tests (to fit its 5th-degree polynomial) than the critical plane.

REFERENCES

1. Socie, D. and Marquis G. (2000) *Multiaxial Fatigue*, SAE International, Warrendale, PA, USA
2. Findley, W.N. (1959). *J Eng Industry* **81**, 301-306.
3. Fatemi, A. and Socie, D. (1988) *Fatigue Fract Eng Mater Struct* **11**, 149-166.
4. Smith, R.N. Watson, P. and Topper, T.H. (1970) *J. of Mater* **5**,767-778.
5. Anes,V., Reis, L. Li, B., Fonte, M. and de Freitas, M. (2014) *International Journal of Fatigue* **6**, 21-33.
6. de Freitas, M., Reis, L. and Li, B. (2006) *Fatigue Fract Eng Mater Struct* **29**, 992-999.